Localization in 3D Surface Sensor Networks: Challenges and Solutions

Yao Zhao, Hongyi Wu, Miao Jin and Su Xia

***Abstract*—This work aims to address the problem of localization in 3D surface wireless sensor networks. First, it reveals the unique hardness in localization on 3D surface in comparison with the well-studied localization problems in 2D and 3D space, and offers useful insight into the necessary conditions to achieve desired localizability. Second, it formulates the localization problem under a practical setting with estimated link distances (between nearby nodes) and nodal height measurements, and introduces a layered approach to promote the localizability of such 3D surface sensor networks. Crossbow sensor-based experiments and large-scale simulations are carried out to evaluate the performance of the proposed localization algorithm. The numeric results show that it can effectively improve localizable rate and achieve low location errors and computational overhead, with the desired tolerability to measurement errors and high scalability to large-size wireless sensor networks.**

I. Introduction

The emerging wireless sensor network technology is opening up tremendous opportunities for ubiquitous monitoring, pervasive computing and autonomous actuation. A sensor network consists of a large number of low cost, resource-constrained sensor nodes, for collaborative data acquisition, processing and communication. Depending on the target application circumstance, a sensor network may be deployed on 2D plane (such as crop fields), 3D volume (e.g., for underwater reconnaissance and atmospheric monitoring), or 3D surface (e.g., in seismic monitoring in mountainous regions), as illustrated in Figs. 1(a)-1(c), respectively.

Geographic location information is imperative to a diversity of applications in wireless sensor networks, ranging from optimal nodal deployment and geometry routing, to position-aware sensing and distributed data storage and retrieval. Although global navigation systems (e.g., GPS) have been widely available for localization, it is often unrealistic or highly cost-ineffective to integrate a GPS receiver in every node of a large-scale sensor network, not to mention its lavishly high energy consumption. Moreover, part or all of the sensors may be prohibited from receiving satellite signals in some application scenarios, rendering it impractical to solely rely on global navigation systems for sensor localization. To this end, GPS-less and GPS-free algorithms have been developed recently for autonomous localization in wireless sensor networks [1]–[24].

A. Review of Autonomous Localization Algorithms

The earliest attempt for localization is based on trilateration. In two-dimensional (2D) geometry, the location of an unknown node can be determined based on the known coordinates of three reference nodes and the precise distances to them, by finding the intersect of three circles centered at the reference nodes. Although absolutely accurate distances are generally unprocurable in practice, the Euclidean distance between two nodes in a wireless sensor network can be estimated by their shortest path with the per hop distance measured by received signal strength indicator (RSSI) or time difference of arrival (TDOA) or simply assumed as a constant. This approach is effective especially when nodal density is sufficiently high and thus the shortest path often approximates a straight line. A straightforward application of trilateration based on such estimated distances may fail to yield a single intersect to localize the unknown node. However, efficient error minimization and fuzzy relaxation techniques such as multi-dimensional scaling (MDS) [15]–[17], nonlinear optimization [20], and neural networks [18], [19] can be adopted to establish coordinates system for practical wireless sensor networks. For example, Fig. 1(d) shows the localization results of MDS, where the distance between two nodes is estimated by their shortest path with the per hop distance assumed as a constant radio range.

The three-dimensional (3D) trilateration is not substantially different from its 2D counterpart [25]. An unknown node can be localized by four reference nodes and the Euclidean distances to them. Moreover, most error minimization algorithms discussed above can be readily extended from 2D to 3D to support practical localization based on estimated distances, although with potentially increased computational complexity. Fig. 1(e) illustrates the localization results based on MDS for the 3D network shown in Fig. 1(b). The above discussions have assumed the shortest path does not detour around a network boundary due to void area. Otherwise, network partition can be applied to diminish the effect of detouring paths [26].

Besides trilateration, a flat metric-based approach [21] has been proposed recently to localize nodes in a distributed manner in wireless sensor networks. It requires estimated local distance between neighboring nodes only, and adopts differential geometry tools to compute flat metrics with minimum deviation from the estimated distances. Then it embeds the network graph according to such flat metrics to yield sensor coordinates. Without the needs of estimating distances between remote nodes, it exhibits high tolerance to complex network settings with concave boundary conditions. However it cannot be readily extended for localization in 3D space.

B. Unique Challenges in Localization on 3D Surface

Given that the aforementioned techniques have solved the problem of localization in sensor networks deployed on 2D

This work is supported in part by National Science Foundation under Award Number CNS-1018306. The authors are with the Center for Advanced Computer Studies, University of Louisiana at Lafayette.

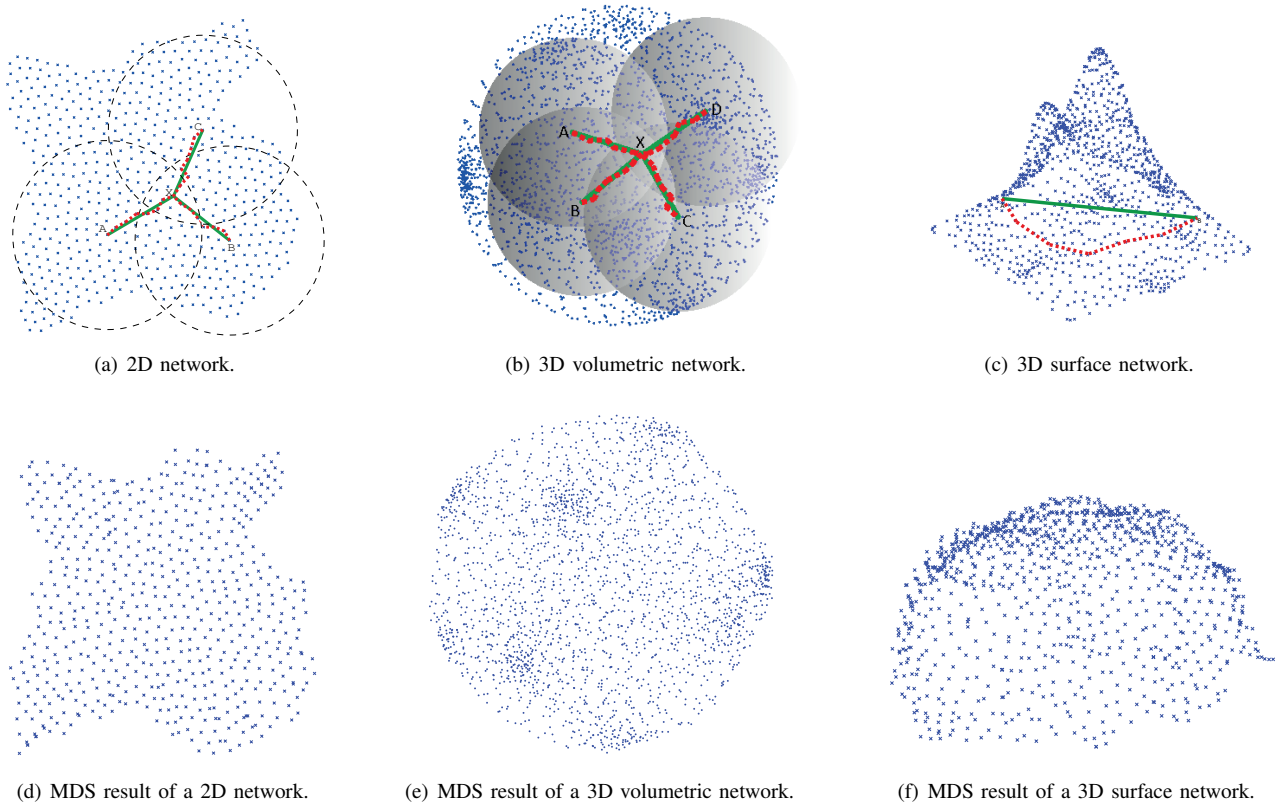

(a) 2D network. (b) 3D volumetric network. (c) 3D surface network.

(d) MDS result of a 2D network. (e) MDS result of a 3D volumetric network. (f) MDS result of a 3D surface network.

Fig. 1. Figs. (a)-(c) illustrate an overview of wireless sensor networks deployed on 2D plane, in 3D volumetric space, and on 3D surface, respectively. The shortest path well approximates the Euclidean distance on 2D plane and in 3D volumetric space, but becomes misleading on 3D surface. Figs. (d)-(f) show the localization results based on MDS, which works well in the 2D network and the 3D volumetric network, but fails in the 3D surface network.

plane or in 3D volumetric space, it appears straightforward at the first glance to apply similar approaches to localize sensor nodes on 3D surface. However, the problem is surprisingly nontrivial due to challenges discussed below, where the essence of the problem is elaborated in a continuous domain.

To facilitate our discussion, we first define the surface distance as follows.

Definition 1: The *surface distance* between two points on a 3D surface is the length of the geodesic connecting them.

Geodesic is a generalization of the notion of a "straight line" to "curved spaces". It is the distance of (locally) the shortest path between the two points on the surface. Our investigation reveals that surface distance constraints are insufficient to localize a general 3D surface. More formally, we establish the following theorem.

Theorem 1: A general 3D surface is not always localizable, given surface distance constraints only.

Proof: A 3D surface is *localizable* if it has a unique embedding up to a global rigid motion, under given constraints. Otherwise it is *non-localizable*.

The theorem can be proven by showing that a 3D surface may have different embeddings in 3D under the assumption of known precise surface distance between any two points on the surface. To this end, examples are constructed to show that a surface can be deformed to another one without changing the surface distance between any pair of points. For instance, a piece of paper (with Gaussian curvature zero everywhere) shown in Fig. 2(a) can be rolled up to a cylinder illustrated in Fig. 2(b) or to other curved shapes (see Fig. 2(c)). The distances between all pairs of points on the paper clearly remain the same under different shapes. Besides the open surface discussed above, similar deformation can be applied on closed surfaces (see Figs. 2(d)-2(f) for example).

Clearly, ambiguous embeddings exist and thus a general 3D surface is not always localizable under given surface distance constraints only. The theorem is thus proven. ■

This result is anti-intuitive as it is commonly assumed that distance information is sufficient for localization, which is, however, untrue for general 3D surfaces as revealed by Theorem 1. As a matter of fact, only a special case of 3D surface is proven localizable based on distance information. More specifically, if the Gaussian curvature of a smooth surface is positive everywhere, the distance information (i.e., metric) can determine an embedding in R^3 as a closed convex surface unique up to a rigid motion or a reflection, given by S. Cohn-Vossen as the rigidity theorem in 1927 [27].

In addition, it is worth to point out that the surface distance between two points is generally different from their Euclidean distance. For example, let's consider a mountainous surface as depicted in Fig. 1(c). The Euclidean distance between Nodes X and Y is shown by the solid green line. However,

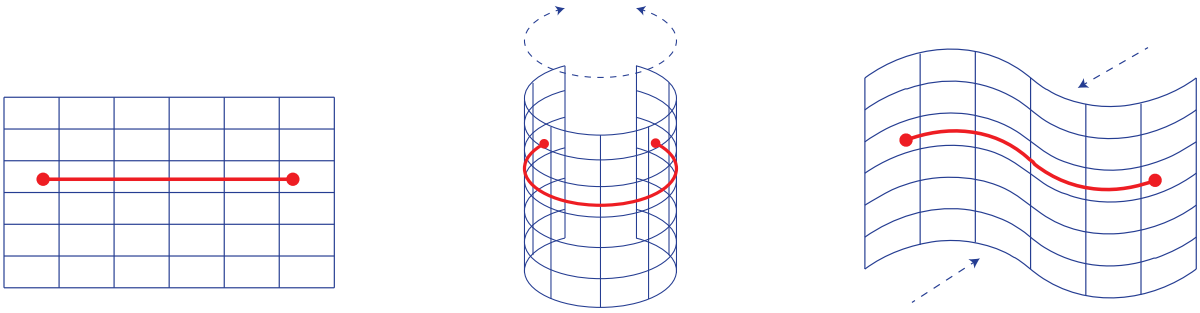

(a) A 2D surface. (b) Deformation to cylinder. (c) Deformation to wave shape.

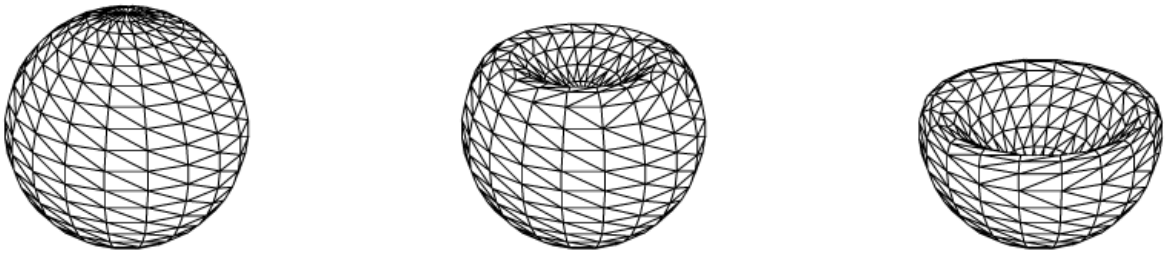

(d) A closed 3D surface. (e) Small deformation. (f) Large deformation.

Fig. 2. Illustration of the non-localizability of general 3D surfaces. A surface can be deformed to another surface without changing the surface distance between any pair of points.

the surface distance between them (see the dashed red line) is dramatically longer. Apparently, there is no deterministic correlation between the Euclidean distance and the surface distance. As a result, it often becomes misleading to estimate the Euclidean distance between two points in a 3D surface sensor network by their shortest path, resulting in extremely high errors or failures under trilateration-based localization (see Fig. 1(f) for example).

C. Contribution of This Work

This work aims to address the problem of localization on 3D surface. Its contributions are twofold:

- First, it reveals the unique hardness in localization on 3D surface (as shown in Theorem 1) and offers useful insight into the necessary conditions to achieve desired localizability.
- Second, it formulates the localization problem under a practical setting with estimated link distances (between nearby nodes) and nodal height measurements, and introduces a layered approach to improve the localizability of such 3D surface sensor networks.

The rest of this paper is organized as follows: Sec. II introduces the proposed localization algorithm. Secs. III and IV present simulation and experimental results, respectively. Sec. V concludes the paper.

II. Proposed Localization Algorithm for 3D Surface Sensor Networks

Following the above theoretic discussions on hardness of localization on a continuous 3D surface, this section focuses on algorithm designed for discrete 3D surface sensor networks. It begins with a formulation of the localization problem under a practical setting with given estimated link distances (between nearby nodes) and nodal height measurements. Although with such augmented input information, the problem is still non-trivial, with only a special case solved. To this end, a layered approach is proposed to improve localizability.

A. Problem Formulation

The objective of this work is to determine locations of sensor nodes deployed on a 3D surface. The 3D surface sensor network has been illustrated in Fig. 1(c). Formally, a 3D surface network is defined as follows.

Definition 2: A *3D surface sensor network* consists of sensor nodes deployed on a 3D surface where wireless signals between nearby nodes propagate along the surface only.

Most discussions and results obtained in a continuous setting in Sec. I-B still hold in a discrete 3D surface sensor network. In a sharp contrast to 3D volumetric sensor networks where the shortest path between two nodes approximates their direct Euclidean distance (see Fig. 1(b)), there is no deterministic correlation between the Euclidean distance and the shortest path in a 3D surface sensor network (as illustrated in Fig. 1(c)). Therefore the trilateration-based schemes often fail. As revealed in Theorem 1, it is intrinsically hard to localize nodes in a general 3D surface network based on surface distances only. To this end, a practical setting with augmented input information is considered in this research, where not only surface distances but also nodal height measurements are

assumed to formulate the localization problem.

Definition 3: For a given sensor network represented by a graph $G = \{V, E\}$, where V is the set of sensor nodes and E is a set of edges between any two neighboring nodes within their radio communication range, the localization problem studied in this research is formulated as follows:

- Input: $\{z_i | i \in V\}$, $\{l_{ij} | ij \in E\}$,
- Output: $\{(x_i, y_i, z_i) | i \in V\}$,

where (x_i, y_i, z_i) are the coordinates of Node i and l_{ij} is the distance between two neighboring nodes i and j.

If the above problem is solved (or can be solved), the network is called *localized* (or *localizable*).

The height (or altitude) of a sensor on a 3D surface is its z-coordinate. It can often be obtained by measuring atmospheric pressure. Such measurement is extremely low cost. As a matter of fact, many sensors have integrated barometer and thus are ready to make atmospheric pressure measurements. For example, the Crossbow MTS400/MTS420 sensor board is equipped with Intersema MS55ER pressure sensor with an error margin of no more than 3.5% in its measured atmospheric pressure and accordingly can determine its height with high accuracy. The height measurements of a 3D surface network are a set of z-coordinates of the sensor nodes on the surface. On the other hand, distance between two neighboring nodes can be estimated by RSSI or more accurate methods if available. Since the sensor's communication range is short, radio signals are generally deemed to propagate along the surface only.

The nodal height measurements help to lower the hardness of the localization problem. One may even expect that the 3D surface localization problem can be reduced to the localization problem on 2D plane with the known nodal height. However, this is anti-intuitively untrue, as demonstrated below.

Theorem 2: A general 3D surface is not always localizable based on surface distance and nodal height information only.

Proof: Given a 3D surface, one can always construct a plane that is parallel to z-axis and intersects the surface. Let S and L denote the surface and the plane, respectively. Obviously, L cuts S into more than one segments. For a segment τ, its mirror image (according to Plane L) is denoted by τ' (as shown in Fig. 3(a)). Accordingly, another surface S' can be constructed based on τ' and the rest segments of S (see Fig. 3(b) for example).

Comparing S and S', it is not difficult to find that any point on S has the same height as its corresponding point on S', because the mirroring is performed according L that is parallel to z-axis. Moreover mirroring does not change surface distances. The surface distance between any two points on S remains the same as its counterpart on S'.

Therefore, a 3D surface does not have a unique embedding and accordingly is not localizable, with given surface distance and nodal height information only. ■

Theorem 2 has revealed the fundamental challenge in localization of a general 3D surface sensor network based on surface distance and nodal height information. The rest of this section first discusses a special 3D surface sensor network, called single-value surface network, which can be localized,

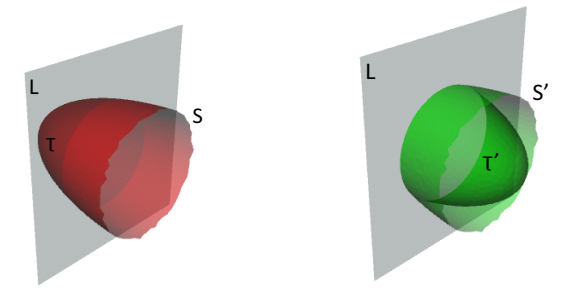

(a) Original surface S. (b) Surface S' after mirroring.

Fig. 3. Illustration of nondeterministics of a 3D surface with given surface distances and nodal height information, where τ' is the mirror image of τ according to Plane L.

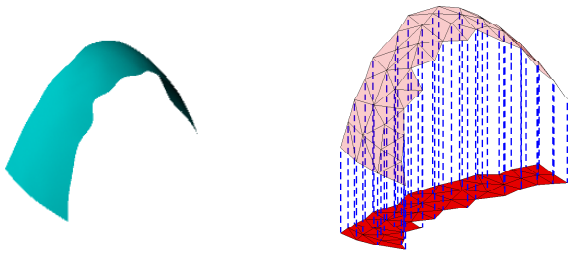

(a) A SV 3D surface network. (b) Triangular mesh and projection.

Fig. 4. Localization of a single-value surface network.

and then introduces a layered approach, aiming to convert a general 3D surface sensor network to a set of single-value surface networks to improve localizability.

B. Localization in Single-Value Surface Networks

Now let's first consider a simplified scenario, i.e., a sensor network deployed on a single-value 3D surface.

Definition 4: A *single-value (SV) 3D surface* is a surface on which any two points have different projections on the x-y plane.

An example of SV 3D surface network is illustrated in Fig. 4(a). The above definition is given in reference to x-y plane since z-coordinate (i.e., nodal height) is assumed available. A general SV surface can be defined according to other planes too, but is not considered in this research. A SV surface is common in many practical applications. For instance, when sensors are airborne to a mountainous region or dropped to underwater seabed, they naturally form a SV 3D surface sensor network.

The localization of a SV 3D surface sensor network follows three steps as outlined below:

- First, based on the connectivity graph of the SV 3D surface sensor network, a distributed algorithm [28] is applied to establish a triangular mesh structure (see Fig. 4(b)). The triangular mesh is a planar graph, where

each non-boundary edge is shared by two and only two triangles.

- Second, the triangular mesh is projected to the x-y plane as illustrated in Fig. 4(b), where the projection of an edge between Node i and Node j has a length of $l'_{ij} = \sqrt{l_{ij}^2 - (z_i - z_j)^2}$. Note that such projection is performed locally by each individual node based on its neighbor information only. The projection is also a triangular mesh.
- Third, based on $\{l'_{ij}|ij \in E\}$ that are subject to errors under a practical sensor network setting, a distributed 2D localization algorithm (e.g., [15]–[21]) is applied to the projected triangular mesh to determine $\{(x_i, y_i)|i \in V\}$. Since z-coordinate is known, each sensor node thus obtains its 3D coordinates (x_i, y_i, z_i).

Lemma 1: A triangulated SV 3D surface sensor network is localizable, given $\{z_i|i \in V\}$ and $\{l_{ij}|ij \in E\}$.

Proof: The above algorithmic procedure serves as a constructive proof for the lemma. ■

If $\{z_i|i \in V\}$ and $\{l_{ij}|ij \in E\}$ are all accurate, the above algorithm yields precise coordinates for the sensor nodes. However, both z_i and l_{ij} are measured with inevitable errors, which consequently lead to inaccurate l'_{ij}, rendering straightforward embedding unviable. The algorithms [15]–[21] adopted for localization essentially produce 2D coordinates $\{(x_i, y_i)|i \in V\}$ with minimized overall errors between l'_{ij} and $\sqrt{(x_i - x_j)^2 + (y_i - y_j)^2}$ $\forall ij \in E$.

C. A Layered Approach for Localization in General 3D Surface Networks

While the localization problem in SV 3D surface sensor networks has been discussed above, there exist a diversity of practical settings that are based on non-single-value (NSV) surfaces.

It is fundamentally challenging to localize a general 3D surface sensor network according to surface distance and nodal height information only as shown by Theorem 2. However Lemma 1 has revealed the desired localizability in a SV 3D surface sensor network. Therefore, a natural step is to convert a general 3D surface sensor network (especially a network deployed on NSV surface) to SV 3D surface sensor networks. To this end, a layered approach is proposed, including layer slicing, localization and suturing as summarized below.

1) Layer Slicing: A general 3D surface is divided into layers. Each layer consists of a set of triangular faces. Let γ_i denote the i^{th} layer. A layer consists of two sublayers of nodes, the lower sublayer γ_i^l and the upper sublayer γ_i^u. Two neighboring layers share a common sublayer, i.e., $\gamma_i^u = \gamma_{i+1}^l$.

The lowest layer, i.e., γ_0, may be constructed in two ways, based on boundary or z-coordinate, respectively. A general 3D surface can be closed or open. An open surface has a boundary. Similar to the first step of the localization algorithm for SV networks, a triangular mesh structure can be established by using a distributed algorithm [28]. Based on the triangular mesh, it is straightforward to identify the boundary of the surface. More specifically, since an internal edge of the triangular mesh is always shared by two neighboring triangles, an edge that is involved in one triangle only is identified as a boundary edge. Consequently, a node on a boundary edge is a boundary node. An arbitrary boundary node can initiate a control packet that only propagates along boundary edges to discover a sequence of boundary edges that form a boundary.

γ_0 can be constructed based on the boundary identified above, comprising all triangular faces that contains at least one boundary node. The boundary nodes form the lower sublayer of γ_0 (i.e., γ_0^l), while the rest nodes in γ_0 are put into γ_0^u. If there exist multiple boundaries, the one with the lowest average z coordinate is chosen. A higher layer is determined by the layer below it. More specifically, if a triangular face contains at least one node in γ_i^u but the face itself is not included in γ_i, it is included into γ_{i+1}. $\gamma_{i+1}^l = \gamma_i^u$, and the rest nodes in γ_{i+1} are put into γ_{i+1}^u. The process repeats until every triangular face is included in a layer.

Alternatively, γ_0^l can be set to the node with the lowest z coordinate, e.g., for the scenario where a 3D surface is closed (as shown in Fig. 5(a)) with no boundary or where the average coordinate of the boundary of an open surface is significantly higher than the lowest z coordinate of the surface. The algorithm remains the same to slice the 3D surface into layers. An example of layer slicing is given in Fig. 5.

2) Layer Localization: By applying the slicing process discussed above, all layers of a sensor network deployed on a SV 3D surface must be SV too. More specifically, we have the following lemma.

Lemma 2: All layers of a SV 3D surface are SV.

Proof: This is obvious by contradiction. If a layer is NSV, there must exist two points on the layer that are projected to the same point on x-y plane. Such two points on the original 3D surface must have the same projection too, which contradicts the given condition that the original 3D surface is SV. Therefore the lemma is proven. ■

The slicing process does not guarantee every layer of a NSV surface to be SV. This is no surprise, because otherwise any NSV surface sensor network would become localizable, contradicting Theorem 2. However, as demonstrated in Fig. 5, the narrow layers are SV with high probability and thus each SV layer can be localized by using the algorithm introduced in Sec. II-B, significantly improving the localizability of 3D surface sensor networks. There exist exceptions where a layer is still NSV. In this case, the NSV layer should be marked as non-localizable, while other localized layers must the properly sutured together under a unified coordinates system as to be discussed next.

3) Layer Suturing: As introduced above, if a 3D surface sensor network is SV, all layers of the network must be SV and localizable. Otherwise given a NSV 3D surface sensor network, the slicing scheme can effectively divide it into layers, which are SV with high probability. In case a layer is still NSV, it should be marked as non-localizable.

The final step of the algorithm is to suture all layers together into a unified coordinates system. The lowest layer, i.e., γ_0,

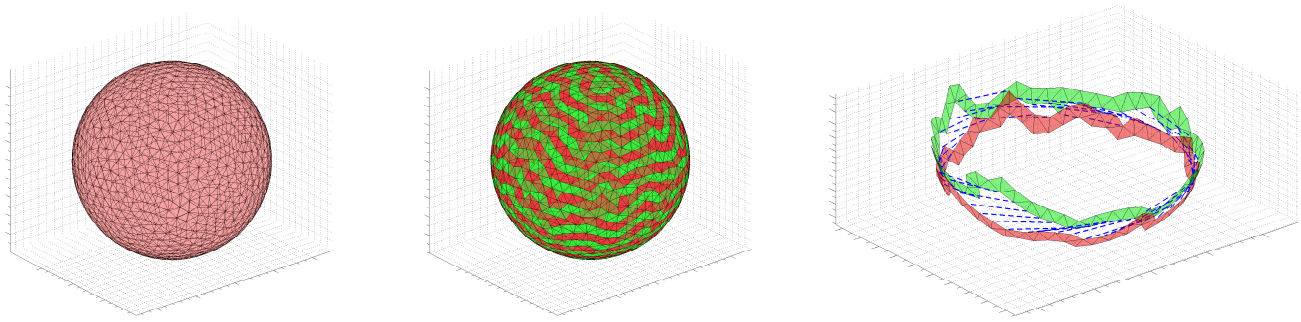

(a) A NSV 3D surface network. (b) Layer slicing. (c) Layer suturing.

Fig. 5. The layer-approach for localization on a NSV 3D surface network.

can determine an arbitrary coordinates system. The suturing process tunes the upper layers based on lower layers to keep nodal coordinates network-wide consistent.

Consider two localized layers, γ_i and γ_j with $j > i$, where γ_i has been sutured to the layer(s) below it and there are no other localized layer(s) between them. The suturing process starts from $i = 0$. If $j = i + 1$, i.e., γ_j and γ_i are adjacent layers, it is straightforward to suture them, because they share a sublayer of nodes, i.e., $\gamma_j^l = \gamma_i^u$, and consequently, the coordinates system used in the lower layer can be propagated to the upper layer.

Challenges stem from the case of $j > i+1$ that indicates one or multiple layers between γ_i and γ_j are non-localizable. Since γ_i and γ_j are localized independently, their coordinate systems are inconsistent. To suture them, the upper layer, i.e., γ_j, must be translated and/or rotated. Given known z-coordinates, such translation and rotation are on x-y plane only, determined by minimizing the Levenberg–Marquardt function:

$$F(dx, dy, \alpha) = \sum_{a \in \gamma_j^l,\ b \in \gamma_i^u} [Y_{ab} - f_{ab}(dx, dy, \alpha)]^2,$$

where dx and dy are translations along the x and y axes and α is rotation that γ_j should apply. For Node a in γ_j^l and Node b in γ_i^u, Y_{ab} is the estimated distance between them (e.g., by the hop count of their shortest path multiplying the average hop distance), and

$$f_{ab}(dx, dy, \alpha) = \sqrt{(x_b - \hat{x}_a)^2 + (y_b - \hat{y}_a)^2},$$

where $\hat{x}_a$ and $\hat{y}_a$ are the new x-y-coordinates of Node a after translation and rotation:

$$\begin{aligned} \hat{x}_a &= x_a \times \cos\alpha - y_a \times \sin\alpha + dx, \\ \hat{y}_a &= x_a \times \sin\alpha + y_a \times \cos\alpha + dy. \end{aligned}$$

Layer γ_j shifts and rotates according to the optimal dx, dy and α that minimize $F(dx, dy, \alpha)$. The above process aligns the two layers such that the overall difference between the estimated surface distance (i.e., Y_{ab}) and the Euclidean distance based on calculated coordinates (i.e., $f(dx, dy, \alpha)$) is minimum. Note that although surface distance is not always correlated with Euclidean distance as revealed in Sec. I-B, it is effective for suturing under most practical settings, where a very small number of NSV layers (often one layer only) exists between γ_i and γ_j. Note that, surface distance is not employed for localization directly. The shapes of γ_i and γ_j have already been fixed, with only three parameters (i.e., dx, dy and α) to be determined. Such constraints diminish the effect of uncorrelated surface distances. The suturing procedure is applied from the lowest to the highest localizable layers such that they are integrated in a consistent coordinate system.

III. Simulation Results

In this section, we present simulation results of the proposed 3D surface localization algorithm under practical network models, to study its performance trend with varying network scales and measurement errors.

A. Simulation Setup

Among a diversity of applications of 3D surface sensor networks, we choose three models inspired by the exploration and monitoring of mountain terrain, sea cave and seismic activities in volcano, as illustrated in Figs. 6(a)-6(c). About one to four thousands of sensor nodes are randomly deployed in each model. The proposed scheme does not rely on specific communication models. For a given communication model, a connectivity graph of the 3D surface sensor network is established. We assume two neighboring nodes can measure the distance between them. Moreover, we assume every node is aware of its height, e.g., via integrated barometer as discussed in Sec. II. Both distance and height are subject to measurement errors, which are varied in our simulations from 0% to 20%. Based on the connectivity graph, a distributed algorithm [28] is applied to establish a triangular mesh structure.

We run the proposed 3D surface localization algorithm using JAVA and MATLAB, including layer slicing, localization and suturing, and evaluate its performance in terms of localizable rate, location error and computational overhead. We assume a general communication model in physical layer in contrast to the nonrealistic UDG or quasi-UDG models [29]. As discussed in Sec. II-C, nodes in NSV layers are marked non-localizable. The localizable rate is the percentage of nodes that can be localized. Based on the localized nodes, we

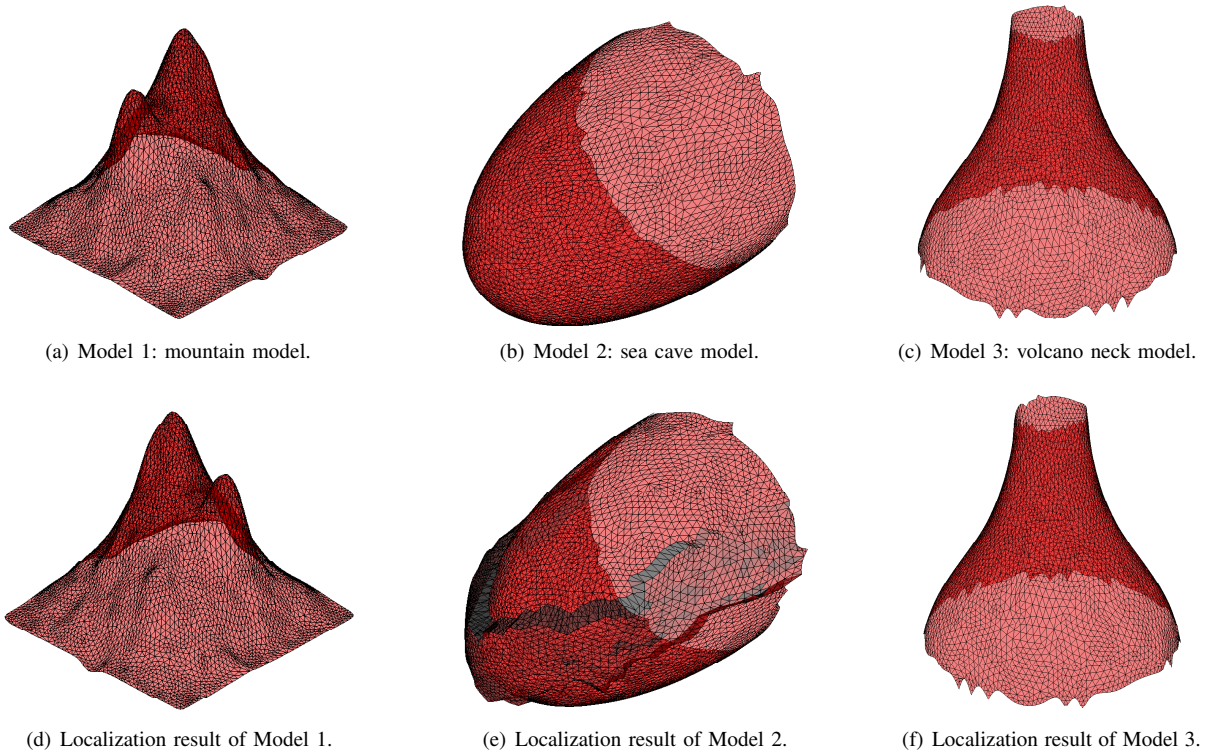

(a) Model 1: mountain model. (b) Model 2: sea cave model. (c) Model 3: volcano neck model.

(d) Localization result of Model 1. (e) Localization result of Model 2. (f) Localization result of Model 3.

Fig. 6. Network models and localization results. The grey color represents localization errors.

calculate location errors that are due to measurement errors in distance and height and the existence of NSV layers. Since the coordinates produced by the localization algorithm often refer to a coordinate system different from the coordinate system used by the ground truth, direct comparison of coordinates is infeasible. To avoid global alignment of coordinates systems, we determine the average location error as follows. Let $l^{'}$ denote the distance between two neighboring nodes computed based on the established coordinates and l denote the ground-truth distance between them. We define the network-wide average of $|l - l^{'}|/r$ to be the average location error, where r is the maximum radio communication range of sensor nodes.

Figs. 6(d)-6(f) depict the localization results under 5% measurement errors. As can be seen, our algorithm can restore origin locations well in general. In Fig. 6(e), the locations of nodes in NSV layers are approximated based on adjacent layers for complete illustration, and thus noticeable deformation can be observed.

B. Localizable Rate

Table I shows the localizable rate under different network models, scales, and measurement errors. The localizable rate is predominantly affected by the NSV layers of a network model, since all nodes in NSV layers are marked non-localizable. As a result, lower localizable rate is observed under the Sea Cave model where multiple middle layers are NSV.

As discussed in Sec. I-A, the distance between two adjacent nodes can be measured by received signal strength indicator (RSSI) or time difference of arrival (TDOA). In practical applications, neither of the two methods yields absolutely precise distance. In our simulations, we assume the distance measurement error is a uniformly distributed random variable and vary the maximum measurement error from 0% to 20% to study its impact on localizable rate. We observe a slightly degraded localizable rate, with the increase of distance errors. This is because distance errors may change geometric characteristics of the 3D surface network and introduce NSV components in an in fact SV layer. The more the measurement errors, the higher the probability to create such NSV components.

In addition, we increase the network size from 1×10^3 to 4×10^3 sensor nodes. The proposed localization algorithm exhibits excellent scalability, with a stable localizable rate unaffected by the network size. As discussed above, the non-localizability is due to the existence of NSV layers, which depends on the geometry shape of the 3D surface itself but is unrelated to network scale or nodal density.

C. Average Location Error

The average location errors are reported in Table II, which are calculated based on localizable nodes only. According to Lemma 1, a SV layer can be precisely located if distance and height measurements are free of errors. This is verified by our simulation results. For SV 3D surfaces (e.g., the Mountain and Volcano models) with zero measurement errors, the localization is perfect, yielding an average location error of zero. It is often expected that the average location error of a NSV 3D surface network must be higher due to the approximation in suturing two non-adjacent layers separated by one or multiple

TABLE I
LOCALIZABLE RATE.

Number of sensors	Maximum measurement error (%)	Mountain (%)	Sea cave (%)	Volcano neck (%)
1×10^3	0	100	91.2	100
	5	99.8	90.9	99.9
	10	99.2	90.3	99.4
	20	98.9	89.4	99.1
2×10^3	0	100	90.4	100
	5	99.9	90.0	99.9
	10	99.7	89.5	99.5
	20	99.1	88.6	98.8
4×10^3	0	100	90.9	100
	5	99.7	90.1	99.9
	10	99.5	89.2	99.7
	20	98.3	88.7	98.6

TABLE II
AVERAGE LOCATION ERROR.

Number of sensors	Maximum measurement error (%)	Mountain (%)	Sea cave (%)	Volcano neck (%)
1×10^3	0	0.00	0.00	0.00
	5	2.53	2.57	2.54
	10	5.70	5.74	5.46
	20	15.9	16.6	13.5
2×10^3	0	0.00	0.00	0.00
	5	2.55	2.58	2.53
	10	5.45	5.69	5.58
	20	16.4	17.8	14.3
4×10^3	0	0.00	0.00	0.00
	5	2.55	2.55	2.53
	10	5.54	5.62	5.43
	20	18.1	15.7	14.0

NSV layers. However, we do not observe a significantly higher localization error in the Sea Cave model, indicating that the suturing procedure effectively tunes different layers to keep nodal coordinates network-wide consistent. This is because, under the set of distance constraints employed in the Levenberg-Marquardt function, there exists little room to yield extra location errors.

With higher measurement errors, the localization results naturally become less accurate. Both the SV and NSV surface networks share the same trend of higher location errors with the increase of measurement error. In addition, similar to our discussion on localizable rate, the network size has no noticeable impact on location errors.

D. Computational Overhead

Given the limited computation, storage and energy resources available at individual sensor nodes, it is highly desirable to achieve low computational overhead in localization, aiming to prolong the lifetime of sensor networks. The proposed algorithm, including layer slicing, localization and suturing, has a time complexity linear to the number of triangles in the triangular mesh structure, if all layers are SV; otherwise, the algorithm needs more iteration runs to suture non-adjacent layers after individual SV layers are localized. Therefore, higher computation overhead is observed under the Sea Cave model as illustrated in Fig. 7.

Fig. 7 also shows that the total computation overhead increases with the network size. This is because a larger network consists of more triangles in its triangular mesh, and thus requires more iterations to complete the localization process. Meanwhile, measurement errors do not noticeably affect computation overhead because they do not change the network structure (especially the number of triangles in the triangular mesh).

IV. EXPERIMENTAL RESULTS

We have also carried out experiment by establishing a 3D wireless sensor network that consists 39 Crossbow MICAz motes. We randomly deploy the motes on the surface of a 3D

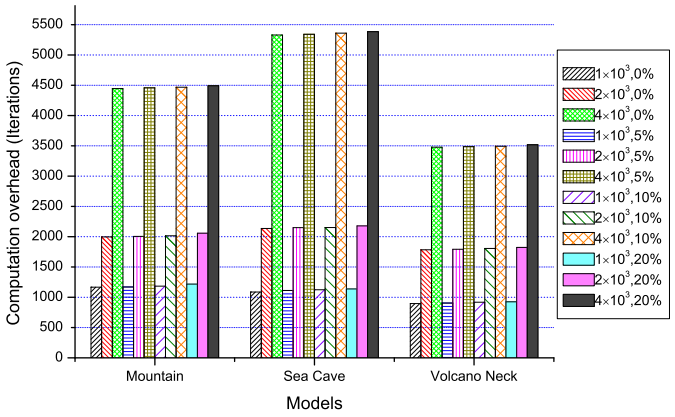

Fig. 7. Computation overhead.

structure, to mimic an airborne network (see Fig. 8(a)). The average distance between two neighboring nodes is approximately $30cm$. The radio transmission distance ranges from $15cm$ to about $50cm$.

We manually measure the positions of the motes with reference to an arbitrary coordinates system which serve as ground truth as illustrated in Fig. 8(b). A line segment between two nodes indicates that they are connected via a wireless link. We use received signal strength indicator (RSSI) to estimate the distance between neighboring nodes. With Crossbow MICAz motes under low transmission power setting, such estimation has an error rate as high as 20%. The localization result is shown in Fig. 8(c). We observe a localizable rate of 100% and an average location error of 13.5% in this experiment. The distance measurement error is the dominating factor that affects the performance of localization.

V. CONCLUSION

We have studied the problem of localization in 3D surface wireless sensor networks. The contributions of this work are twofold. First, our investigation has revealed the unique hardness in localization on 3D surface in comparison with the well-studied localization problems in 2D and 3D space,

(a) Experiment setup.

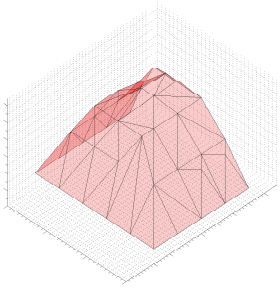

(b) Ground truth.

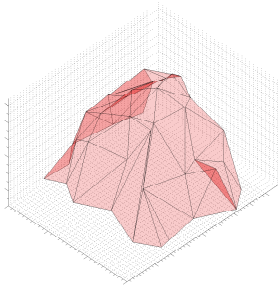

(c) Localization result.

Fig. 8. Experimental setup and results.

and offered useful insight into the necessary conditions to achieve desired localizability. Second, we have formulated the localization problem under a practical setting with estimated link distances (between nearby nodes) and nodal height measurements. We have introduced a layered approach to improve the localizability of such 3D surface sensor networks. We have carried out experiments based on Crossbow motes and performed large-scale simulations to evaluate the performance of the proposed localization algorithm. Our simulation results have shown that it can effectively improve localizable rate and achieve low location errors and computational overhead, with the desired tolerability to measurement errors and high scalability to large-size wireless sensor networks.

REFERENCES

[1] N. Bulusu, J. Heidemann, and D. Estrin, "GPS-less Low Cost Outdoor Localization For Very Small Devices," *IEEE Personal Communications Magazine*, vol. 7, no. 5, pp. 28–34, 2000.

[2] A. Savvides, C. Han, and M. B. Strivastava, "Dynamic Fine-Grained Localization in Ad-Hoc Networks of Sensors," in *Proc. of MobiCom*, pp. 166–179, 2001.

[3] J. Albowicz, A. Chen, and L. Zhang, "Recursive Position Estimation in Sensor Networks," in *Proc. of ICNP*, pp. 35–41, 2001.

[4] L. Doherty, L. Ghaoui, and K. Pister, "Convex Position Estimation in Wireless Sensor Networks," in *Proc. of INFOCOM*, pp. 1655–1663, 2001.

[5] T. He, C. Huang, B. Blum, J. Stankovic, and T. Abdelzaher, "Range-free Localization Schemes in Large Scale Sensor Networks," in *Proc. of MobiCom*, pp. 81–95, 2003.

[6] D. Niculescu and B. Nath, "Ad Hoc Positioning System (APS)," in *Proc. of GLOBECOM*, pp. 2926–2931, 2001.

[7] C. Savarese and J. Rabaey, "Robust Positioning Algorithms for Distributed Ad-Hoc Wireless Sensor Networks," in *Proc. of USENIX Annual Technical Conference*, pp. 317–327, 2002.

[8] A. Nasipuri and K. Li, "A Directionality Based Location Discovery Scheme for Wireless Sensor Networks," in *Proc. of ACM International Workshop on Wireless Sensor Networks and Applications*, pp. 105–111, 2002.

[9] D. Niculescu and B. Nath, "Ad Hoc Positioning System (APS) Using AOA," in *Proc. of INFOCOM*, pp. 1734–1743, 2003.

[10] H. S. AbdelSalam and S. Olariu, "Passive Localization Using Rotating Anchor Pairs in Wireless Sensor Networks," in *Proc. of The 2nd ACM International Workshop on Foundations of Wireless Ad Hoc and Sensor Networking*, pp. 67–76, 2009.

[11] Z. Zhong and T. He, "MSP: Multi-Sequence Positioning of Wireless Sensor Nodes," in *Proc. of SenSys*, pp. 15–28, 2007.

[12] J. Aspnes, T. Eren, D. K. Goldenberg, A. S. Morse, W. Whiteley, Y. R. Yang, B. D. O. Anderson, and P. N. Belhumeur, "A Theory of Network Localization," *IEEE Transactions on Mobile Computing*, vol. 5, no. 12, pp. 1663–1678, 2006.

[13] K. Yedavalli and B. Krishnamachari, "Sequence-Based Localization in Wireless Sensor Networks," *IEEE Transactions on Mobile Computing*, vol. 7, no. 1, pp. 81–94, 2008.

[14] S. Capkun, M. Hamdi, and J. Hubaux, "GPS-Free Positioning in Mobile Ad-Hoc Networks," in *Proc. of The 34th Annual Hawaii International Conference on System Sciences*, pp. 3481–3490, 2001.

[15] Y. Shang, W. Ruml, Y. Zhang, and M. P. J. Fromherz, "Localization from Mere Connectivity," in *Proc. of MobiHoc*, pp. 201–212, 2003.

[16] Y. Shang and W. Ruml, "Improved MDS-based Localization," in *Proc. of INFOCOM*, pp. 2640–2651, 2004.

[17] V. Vivekanandan and V. W. S. Wong, "Ordinal MDS-based Localization for Wireless Sensor Networks," *International Journal of Sensor Networks*, vol. 1, no. 3/4, pp. 169–178, 2006.

[18] G. Giorgetti, S. Gupta, and G. Manes, "Wireless Localization Using Self-Organizing Maps," in *Proc. of IPSN*, pp. 293 – 302, 2007.

[19] L. Li and T. Kunz, "Localization Applying An Efficient Neural Network Mapping," in *Proc. of The 1st International Conference on Autonomic Computing and Communication Systems*, pp. 1–9, 2007.

[20] H. Wu, C. Wang, and N.-F. Tzeng, "Novel Self-Configurable Positioning Technique for Multi-hop Wireless Networks," *IEEE/ACM Transactions on Networking*, vol. 13, no. 3, pp. 609–621, 2005.

[21] M. Jin, S. Xia, H. Wu, and X. Gu, "Scalable and Fully Distributed Localization With Mere Connectivity," in *Proc. of INFOCOM*, 2011.

[22] J. Wang, M. Tian, T. Zhao, and W. Yan, "A GPS-Free Wireless Mesh Network Localization Approach," in *Proc. of International Conference on Communications and Mobile Computing*, pp. 444–453, 2009.

[23] R. Magnani and K. K. Leung, "Self-Organized, Scalable GPS-Free Localization of Wireless Sensors," in *Proc. of WCNC*, pp. 3798–3803, 2008.

[24] H. Akcan, V. Kriakov, H. Bronnimann, and A. Delis, "GPS-Free Node Localization in Mobile Wireless Sensor Networks," in *Proc. of The 5th ACM International Workshop on Data Engineering for Wireless and Mobile Access*, pp. 35–42, 2006.

[25] J. Wang, Y. Chen, X. Fu, J. Wang, W. Yu, and N. Zhang, "3DLoc: Three Dimensional Wireless Localization Toolkit," in *Proc. of ICDCS*, pp. 30–39, 2010.

[26] G. Tan, M. Bertier, and A.-M. Kermarrec, "Convex Partition of Sensor Networks and Its Use in Virtual Coordinate Geographic Routing," in *Proc. of INFOCOM*, pp. 1746–1755, 2009.

[27] S. Cohn-Vossen, "Zwei Sätze über die Starrheit der Einflächen," *Nachr. Ges. Wiss. Göttingen Math.-Phys. Kl.*, 1927.

[28] H. Zhou, H. Wu, S. Xia, M. Jin, and N. Ding, "A Distributed Triangulation Algorithm for Wireless Sensor Networks on 2D and 3D Surface," in *Proc. of INFOCOM*, 2011.

[29] F. Kuhn and A. Zollinger, "Ad-hoc Networks Beyond Unit Disk Graphs," in *Proc. of ACM SIGACT/SIGMOBILE International Workshop on Foundations of Mobile Computing*, pp. 69–78, 2003.